
Article:
Spragg, J orcid.org/0000-0002-0300-2672, Mahmud, T and Dupont, V orcid.org/0000-0002-3750-0266 (2018) Hydrogen production from bio-oil: a thermodynamic analysis of sorption-enhanced chemical looping steam reforming. International Journal of Hydrogen Energy, 43 (49). pp. 22032-22045. ISSN 0360-3199

https://doi.org/10.1016/j.ijhydene.2018.10.068

Accepted in International Journal of Hydrogen Energy on 9th October 2018

Hydrogen production from bio-oil: a thermodynamic analysis of sorption-enhanced chemical looping steam reforming

J. Spragg*, T Mahmud, V. Dupont

School of Chemical and Process Engineering, University of Leeds, LS2 9JT, UK

Abstract

The steam reforming of pyrolysis bio-oil is one proposed route to low carbon hydrogen production, which may be enhanced by combination with advanced steam reforming techniques. The advanced reforming of bio-oil is investigated via a thermodynamic analysis based on the minimisation of Gibbs Energy. Conventional steam reforming (C-SR) is assessed alongside Sorption Enhanced Steam Reforming (SE-SR), Chemical Looping Steam Reforming (CLSR) and Sorption Enhanced Chemical Looping Steam Reforming (SE-CLSR). The selected CO_2 sorbent is CaO(s) and oxygen transfer material (OTM) is Ni/NiO. PEFB bio-oil is modelled as a surrogate mixture and two common model compounds, acetic acid and furfural, are also considered. A process comparison highlights the advantages of sorption-enhancement and chemical looping, including improved purity and yield, and reductions in carbon deposition and process net energy balance.

The operating regime of SE-CLSR is evaluated in order to assess the impact of S/C ratio, NiO/C ratio, CaO/C ratio and temperature. Autothermal operation can be achieved for S/C ratios between 1 and 3. In autothermal operation at 30 bar, S/C ratio of 2 gives a yield of 11.8wt%, and hydrogen purity of 96.9mol%. Alternatively, if autothermal operation is not a priority, the yield can be improved by reducing the quantity of OTM. The thermodynamic analysis highlights the role of advanced reforming techniques in enhancing the potential of bio-oil as a source of hydrogen.

Keywords

Bio-oil; Steam reforming; Chemical looping; Sorption enhancement; Thermodynamic analysis

1. Introduction

Hydrogen is an important chemical feedstock for various applications, including the chemicals sector, crude oil refining and fertiliser manufacture [1].There is also interest in hydrogen as a clean energy vector for a range of applications, including transport, heating and energy storage [2,3]. As the energy system is undergoing considerable transition, the nature of the future energy mix remains unclear, but it is evident that hydrogen use can be expected to grow in a number of sectors [4,5].

Most hydrogen is produced by the steam reforming of fossil fuels [6]. The steam reforming reaction releases hydrogen from the fuel, but also releases carbon in the form of CO_2. Further CO_2 is released from fuel combustion, which is required to heat the endothermic reaction. As a result, steam methane

* Corresponding author.

E-mail address: pmjss@leeds.ac.uk (J. Spragg)

reforming releases around 10 to 12 kg CO_2 for each kg of H_2 produced [7,8]. Annual global emissions from hydrogen production are around 500 megatonnes CO_2 per year [5], which was equivalent to approximately 1.4% of the total CO_2 emissions from fossil fuels and industry in 2016 [9]. To continue to meet hydrogen demand within a decarbonised economy, it is necessary to establish low carbon methods of hydrogen production on a large scale.

While life cycle assessment has shown that fossil fuel steam reforming has a high carbon footprint compared to other hydrogen production methods, the process is capable of producing hydrogen cost-effectively and efficiently at large scale [10]. If steam reforming could be combined with methods to reduce emissions, such as low carbon feedstocks and Carbon Capture Utilisation and Storage (CCUS), it may be a promising solution for efficient, large scale production of low carbon hydrogen.

One means of reducing the carbon emissions, as well as reducing dependence on fossil fuels, is to use a feedstock derived from bioenergy. There are multiple methods to convert the hydrogen-containing compounds within biomass to hydrogen. One method uses pyrolysis to convert solid biomass into bio-oil, which is subsequently used in a steam reforming process. Bio-oil is an energy-dense liquid containing a complex mixture of oxygenated organic compounds. It can be transported as a liquid fuel, potentially enabling a network of decentralised pyrolysis plants which serve a central steam reforming facility [1]. Bio-oil steam reforming can reduce greenhouse gas emissions by around 50% compared to natural gas, depending on the source of the biomass [11].

Experimental studies of bio-oil steam reforming have demonstrated bio-oil conversions of over 90%, but highlighted that carbon deposition is a challenge for this chemically complex feedstock [12]. The risk of carbon deposition may be partly alleviated by catalyst selection. Low cost nickel-based catalysts are capable of breaking the C-C bonds in the bio-oil, and have high activity for steam reforming, but they are also very active for coke formation and methanation. Noble metals have demonstrated higher reforming activities and reduced carbon deposition, but the cost can be prohibitive. Another approach includes modifying Ni-based catalysts with promoters, including metals such as Cu, Co and Zn, or metal oxides such as La_2O_3, MgO and CaO [13,14].

Steam reforming may also be improved using advanced process techniques, such as sorption enhancement and chemical looping. In Sorption-Enhanced Steam Reforming (SE-SR), the reaction is enhanced by the addition of a solid CO_2 sorbent [15]. The sorbent removes CO_2 from the reactor, enhancing purity and enabling in situ CO_2 capture. At the same time, it shifts the chemical equilibrium, thereby improving hydrogen yield. A range of sorbents have been studied, including MgO, hydrotalcite, Li_2O_3 and alkaline ceramics. CaO has been identified as a promising sorbent with high capacity and low cost, although long-term stability remains a challenge [16,17].

In chemical looping steam reforming (CLSR), an oxygen transfer material (OTM) provides an undiluted source of oxygen for partial oxidation of the fuel, thereby enabling an autothermal reforming process without costly air separation [18]. It is closely related to other chemical looping processes proposed for hydrogen production, such as steam reforming with chemical looping combustion (SR-CLC), or chemical looping water splitting [19–23].

Early studies such as those by Fathi et al. [24] and Rydén et al. [25] demonstrated the feasibility of CLSR. Over 700 OTMs have since been developed and tested for combustion and reforming [19], aiming to produce materials with high catalytic activity and stability [26–29]. OTMs are typically comprised of a metal oxide such as Cu, Fe_2O_3, NiO, or Mn_3O_4 supported on an inert material such as Al_2O_3, $MgAl_2O_4$, SiO_2, TiO_2 or ZrO_2 [30]. Nickel-based OTMs are the most extensively analysed in literature [19] and have the crucial advantage in packed bed configuration of being the best steam reforming catalysts in their reduced, metallic form. Studies with methane and Ni/NiO have demonstrated high reactivity and stability at high temperatures, as well as high selectivity towards hydrogen production [28,30–32]. The CLSR concept has also been applied to alternative fuels from bioenergy sources, including glycerol [33,34], waste lubricating oil [35], and bioethanol [36]. This also includes the CLSR of bio-oil and its model compounds on nickel-based OTMs [37–39].

The advantages of sorption enhancement and chemical looping can be combined into SE-CLSR, to give high purity hydrogen in an autothermal process [32,40–42]. Recent work has demonstrated the performance of acetic acid in SE-CLSR, as a model compound for bio-oil [43]. Over 20 successive cycles at 923K, the yield remained above 78% of the equilibrium value.

These results suggest that there is an opportunity to combine advanced reforming techniques with bio-based feedstocks. The advantages of advanced reforming techniques, such as improved yields, efficiencies and flexibility of scale, could strengthen the technical and economic case for the uptake of alternative feedstocks. At the same time, there are advantages to developing the next generation of steam reforming techniques in parallel with an understanding of future fuels. In particular, enabling cost-effective carbon capture in bio-oil steam reforming would unlock a new type of bioenergy with carbon capture and storage (BECCS), which has been identified as a vitally important source of negative emissions [44].

In this study, a thermodynamic analysis is carried out to evaluate hydrogen production from bio-oil. Thermodynamic analysis is an informative tool which can be used to evaluate key process parameters such as equilibrium yields, conversions and the energy balance. It is a first step towards more realistic, dynamic models, capable of simulating real processes and demonstrating real improvements over conventional steam reforming of fossil fuels. This technique has been used to investigate advanced reforming of several feedstocks, including methane [42,45], shale gas [41] and glycerol [46]. Thermodynamic analysis has also been carried out on bio-oil model compounds in conventional steam reforming, SE-SR and CLSR [47–50].

Two opportunities have been identified to improve understanding of the advanced reforming of bio-oil. First is the study of SE-CLSR, which has not previously been examined for bio-oil. Second is the modelling of bio-oil as a mixture of compounds, rather than a single model compound, to give a closer assessment of its potential. This work examines three feedstocks relating to bio-oil: a bio-oil surrogate mixture, and two model compounds. The steam reforming techniques studied include conventional steam reforming (C-SR), sorption-enhanced steam reforming (SE-SR), chemical looping steam reforming (CLSR), and sorption-enhanced chemical looping steam reforming (SE-CLSR).

Thermodynamic analysis is applied to evaluate an approximate energy balance of bio-oil reforming processes, as well as the hydrogen yield, product purity, and potential for carbon deposition. The autothermal operation of SE-CLSR is assessed, to identify opportunities for optimisation. Given the high oxygen content of bio-oils and lower calorific value, important questions addressed in this study are whether sufficient heat can be generated by the unmixed oxidation of the bio-oil surrogate mixture and the two model compounds to supply the demand of their steam reforming, and whether the requirement for sorbent material does not overwhelm the heat balance due to larger CO_2 generation, both necessary to maintain cyclic operation.

2. Process description

In conventional steam reforming (C-SR), a hydrocarbon or other organic fuel reacts with steam to produce hydrogen and carbon dioxide (R1 to R3 in Table 1). In industry, the reaction typically occurs in two reactor stages: a reforming stage and a water gas shift (WGS) stage. The reforming reactor performs the endothermic R1 at high temperature, producing syngas. The WGS reactor reduces the carbon monoxide content via the exothermic R2, increasing H_2 yield and purity [51]. This study focusses on the high temperature reforming stage.

Three advanced reforming processes are also considered: SE-SR, CLSR and SE-CLSR. In SE-SR, a CO_2 sorbent is added to the reforming reactor. The sorption of CO_2 shifts the chemical equilibrium and provides heat, resulting in improved yield and purity, as well as achieving in situ capture of CO_2 [15]. In CLSR, an oxygen transfer material (OTM), typically a metal oxide, provides oxygen for partial oxidation of the fuel (R9). In its reduced form, the OTM acts as a catalyst for the reforming reaction, so that fuel oxidation in the absence of air occurs simultaneously with reforming. The release of heat from fuel oxidation reduces energy demand, so that the reformer may be autothermal, and no longer requires indirect heating from a furnace. The OTM provides oxygen in an undiluted form, thereby eliminating the need for costly air separation [18]. SE-CLSR combines sorption enhancement with the chemical looping principle, bringing about added benefits through combination of equilibrium shift, steam reforming and OTM reduction.

To enable regeneration of sorbent and re-oxidation of the OTM, these advanced reforming processes are cyclical. The cycle steps can occur in a series of fluidised beds, or within a packed bed with sequenced flows [30,52]. The cycles of SE-SR, CLSR and SE-CLSR in a packed bed have previously been illustrated in S G Adiya et al [41].

In these processes, steam reforming occurs alongside reactions of the OTM and sorbent. In addition, a number of reactions lead to coke formation [53]. Table 1 shows the generalised reaction scheme for an organic compound $C_nH_mO_k$. On the basis of the literature review, the selected OTM is Ni/NiO. The selected CO_2 sorbent is $CaO_{(s)}$.

Table 1 - Main reactions in sorption-enhanced and chemical looping reforming of an organic compound $C_nH_mO_k$

No.	Reaction	Description
R1	$C_nH_mO_k + (1-k)H_2O \leftrightarrow CO + (\frac{m}{2} - k + 1)H_2$	Steam reforming
R2	$CO + H_2O \leftrightarrow CO_2 + H_2$	Water gas shift
R3	$C_nH_mO_k + (2n-k)H_2O \leftrightarrow nCO_2 + (2n + \frac{m}{2} - k)H_2$	Global steam reforming
R4	$CO + 3H_2 \leftrightarrow CH_4 + H_2O$	Methanation
R5	$CO_2 + 4H_2 \leftrightarrow CH_4 + 2H_2O$	Methanation
R6	$CaO_{(s)} + CO_2 \leftrightarrow CaCO_{3(s)}$	Carbonation of $CaO_{(s)}$
R7	$CaO_{(s)} + H_2O \leftrightarrow Ca(OH)_{2\,(s)}$	Hydration of $CaO_{(s)}$
R8	$C_nH_mO_k + (2n-k)H_2O + nCaO \rightarrow nCaCO_3 + (2n + \frac{m}{2} - k)H_2$	Sorption-enhanced steam reforming
R9	$C_nH_mO_k + \left(\frac{3n}{2} - k\right)NiO \rightarrow \left(\frac{3n}{2} - k\right)Ni + \frac{n}{2}CO + \frac{n}{2}CO_2 + \frac{m}{2}H_2$	Reduction of NiO/oxidation of fuel
R10	$C_nH_mO_k + \left(n - \frac{2k}{3}\right)NiO + (n - \frac{k}{3})H_2O \rightarrow \left(n - \frac{2k}{3}\right)Ni + nCO_2 + (n + \frac{m}{2} - \frac{k}{3})H_2$	CLSR (combined NiO reduction and global steam reforming).
R11	$C_nH_mO_k + \left(n - \frac{2k}{3}\right)NiO + \left(n - \frac{k}{3}\right)H_2O + nCaO \rightarrow \left(n - \frac{2k}{3}\right)Ni + nCaCO_3 + (n + \frac{m}{2} - \frac{k}{3})H_2$	SE-CLSR (combined NiO reduction and sorption-enhanced steam reforming)
R12	$Ni_{(s)} + 0.5O_2 \rightarrow NiO_{(s)}$	Oxidation of Ni
R13	$C_nH_mO_k \leftrightarrow C_xH_yO_z + gases\ (H_2, H_2O, CO, CO_2, CH_4 \ldots) + coke$	Thermal pyrolysis reaction
R14	$2CO \leftrightarrow CO_2 + C$	Boudouard reaction
R15	$CO + H_2 \leftrightarrow C + H_2O$	Coke formation from CO
R16	$CH_4 \leftrightarrow C + 2H_2$	Coke formation from CH_4

3. Methodology

3.1. Energy balance

Fig. 1 illustrates the main components in the energy balance for the SE-CLSR process. As well as the heat associated with reactions, the balance also includes heating of reactants, and heat recuperation from the solids and waste gases.

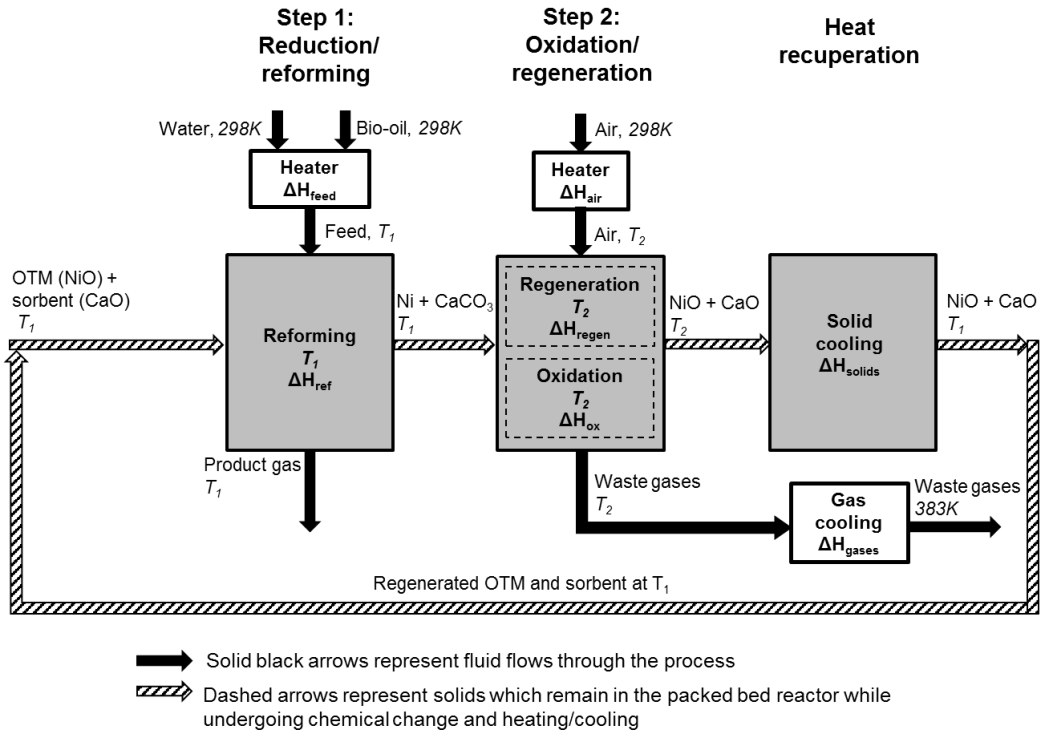

Fig. 1. Schematic description of SE-CLSR, showing key energy terms and temperature assumptions.

The ΔH terms were based on the definitions given in [41]. In this study, they are defined as:

ΔH_{feed} is the enthalpy change required to raise liquid reactants from 298K to reforming temperature (T_1).

ΔH_{ref} is the enthalpy associated with the reactions in the reduction/reforming step, occurring isothermally at T_1.

ΔH_{regen} is the enthalpy associated with sorbent regeneration, including the heating of the sorbent from T_1 to T_2, and the enthalpy of reaction. For a 1.013 bar system, the regeneration temperature was set at 1170K. For higher pressure systems, the temperature was raised to ensure full regeneration of the sorbent. T_2 is 1240K, 1300K and 1420K for a 5 bar, 10 bar and 30 bar system respectively.

ΔH_{air} is the enthalpy change required to heat air from 298K to regeneration/oxidation temperature (T_2).

ΔH_{ox} is the enthalpy released by oxidation of Ni, at T_2. Where there is solid carbon present in the equilibrium products, ΔH_{ox} also includes the oxidation of this carbon.

ΔH_{solids} is the enthalpy change associated with heating or cooling the regenerated solids (NiO and CaO) from T_2 to reformer temperature (T_1), so that they are returned to the starting point of the next cycle.

ΔH_{gases} is the heat recuperated from cooling the waste gases from step 2. This includes unreacted N_2 from the air, and the CO_2 released by sorbent regeneration. Gases are cooled from T_2 to 383K.

ΔH_{total} is the overall energy balance, calculated as the sum of all the energy terms.

For C-SR: $\Delta H_{total} = \Delta H_{feed} + \Delta H_{ref}$

For SE-SR: $\Delta H_{total} = \Delta H_{feed} + \Delta H_{ref} + \Delta H_{regen} + \Delta H_{solids} + \Delta H_{gases}$

For CLSR: $\Delta H_{total} = \Delta H_{feed} + \Delta H_{ref} + \Delta H_{air} + \Delta H_{ox} + \Delta H_{solids} + \Delta H_{gases}$

For SE-CLSR: $\Delta H_{total} = \Delta H_{feed} + \Delta H_{ref} + \Delta H_{air} + \Delta H_{ox} + \Delta H_{regen} + \Delta H_{solids} + \Delta H_{gases}$

Where a unit was exothermic, this was signified by a negative energy term. Where ΔH_{total} was equal to or less than zero, the process as a whole is autothermal.

An Aspen Plus simulation was used to calculate the terms in the energy balance. Reactors were modelled using RGibbs reactor blocks, which calculate thermodynamic equilibrium by the minimisation of Gibbs free energy. The selected property method was Peng-Robinson [54]. A series of two reactors, with the solids flowing from one reactor to another, was used to represent the two main cycle stages. In C-SR, SE-SR and CLSR, the absence of OTM or sorbent was modelled by setting the flow of the corresponding stream to zero.

To assess the potential for carbon deposition, solid carbon (graphite) was included as a component within Aspen Plus. Fluid inputs (fuel, water, air) enter the system at 298K, and at operating pressure. The energy balance did not include the energy required to raise the fluids to this pressure, or any other electrical or auxiliary energy. The flow of air was set by a calculator block, which calculated the stoichiometric quantity of air required to completely oxidise the nickel. The composition of air was assumed as 79% N_2 and 21% O_2.

Key process parameters are the steam-to-carbon (S/C) ratio, NiO to carbon (NiO/C) ratio and sorbent to carbon (CaO/C) ratio. The flow of steam, Ni and CaO were set using a calculator block, which multiplied the molar carbon flow by the relevant ratio. For S/C ratio, the calculation took account for the water content in the bio-oil:

$$n_{steam} = \left(\sum \alpha_i n_{C,bio-oil} \times S\right) - y_{H_2O} n_{bio-oil}$$

Where n_{steam} and $n_{bio-oil}$ are the molar flow rates of steam and bio-oil respectively. S is the S/C ratio, y_{H_2O} is the molar fraction of water in bio-oil, $n_{C,bio-oil}$ represents the number of moles of carbon species in the bio-oil, and α_i is the number of carbon atoms in the carbon species.

The yield was expressed as wt% of the feedstock. As the bio-oil has a high moisture content (Table 2), the yield was expressed on a wet basis and moisture-free (m.f.) basis:

$$H_2\ yield\ (wt\%, \text{wet}) = \frac{n_{H_2} \times MW_{H_2}}{n_{fuel,wet} \times MW_{wet}} \times 100$$

$$H_2\ yield\ (wt\%, \text{m.f.}) = \frac{n_{H_2} \times MW_{H_2}}{n_{fuel,m.f.} \times MW_{m.f.}} \times 100$$

Where n_{H_2} is the number of moles of hydrogen produced, and MW_{H_2} is the molecular weight of hydrogen. $n_{fuel,wet}$ represents the number of moles of fuel including moisture content, and MW_{wet} is its molecular mass. $n_{fuel,m.f.}$ is the number of moles of the organic fraction of the fuel, and $MW_{m.f.}$ is its molecular mass.

The yield was also expressed as a percentage of the theoretical potential from the SE-CLSR global reaction (R11):

$$H_2\ yield\ (\%\ of\ stoich.potential) = \frac{mol\ H_2\ produced}{mol\ H_2\ from\ SE\text{-}CLSR\ stoichiometry} \times 100$$

Purity was calculated as the molar percentage of hydrogen in the product gas, on a dry basis:

$$H_2\ purity\ (mol\ \%) = \frac{n_{H_2,product}}{n_{total,product} - n_{H_2O,product}} \times 100$$

Where $n_{i,product}$ is the number of moles of component i in the product gas.

3.2. Feedstocks

Three different feedstocks were considered: acetic acid, furfural, and bio-oil surrogate mixture. Bio-oil has a complex chemical composition, which varies between different feedstocks and processes [55], so that studies commonly used a single model compound as an approximation. Acetic acid is often used, as it is one of the most abundant compounds found in compositional analysis [12,56–58]. In this study, furfural was also selected because its molecular formula ($C_5H_4O_2$) closely matches that of the moisture-free bio-oil model mixture shown in Table 3. Furfural has been used as a model compound by several authors [38,59]. Remón et al [60] used a statistical analysis to identify that acetic acid and furfural were the compounds which had the most significant effect on bio-oil reforming performance.

Bio-oil may also be simulated by a mixture of components, using a variety of approaches. Plou et al. [61] used mixtures of acetic acid, methanol and acetol to represent three major groups in bio-oil (acids, alcohols and ketones). Other authors have matched their mixture composition to a detailed compositional analysis, using around 10 different compounds [62,63]. An alternative approach involves using a selection of model compounds, in combinations that give an elemental composition ($C_nH_mO_k$) matching that of a real bio-oil [64,65].

In this study, the composition of the bio-oil surrogate mixture was based on the work of Dupont et al. [66]. The bio-oil is represented as a mixture of the 6 macro-families identified by Garcia-Perez et al. [67]. The mass fraction of each compound was selected using curve fitting procedures, in order that the elemental composition and differential thermogravimetric (DTG) curve closely matches that of a real Palm Empty Fruit Bunch (PEFB) bio-oil [68]. A sensitivity analysis on PEFB bio-oil model mixtures has previously shown that the equilibrium results are not sensitive to the exact mixture composition, provided that the elemental composition is known [69]. The composition used in this study is shown in Table 2.

Table 2 – PEFB bio-oil model mixture composition[66,70]

		C	H	O
Ultimate analysis, mol fraction [a]		0.286	0.491	0.223
Model mixture, mol fraction		0.268	0.519	0.213
Percentage of error, %		6.2	5.8	4.8
Water, wt.% [a]		24.3		
Model water, wt.%		24.0		
Family[b]	Family wt.%	Model compounds	Mass fraction	
1	F1=10%	Formaldehyde, CH_2O	0.08	
		Acetaldehyde, C_2H_4O	0.01	
		1-hydroxy-2-butanone, $C_4H_8O_2$	0.01	
2	F2=30%	Acetic acid, $C_2H_4O_2$	0.07	
		Water, H_2O	0.23	
3	F3=15%	Furfural, $C_5H_4O_2$	0.13	
		Phenol, C_6H_6O	0.01	
		Water, H_2O	0.01	
4	F4=15%	Creosol, $C_8H_{10}O_2$	0.14	
		Guaiacol, $C_7H_8O_2$	0.01	
5	F5+F6=30%	Catechol, $C_6H_6O_2$	0.24	
6		Palmitic acid, $C_{16}H_{32}O_2$	0.01	
		Levoglucosan, $C_6H_{10}O_5$	0.05	

[a] Composition of real PEFB bio-oil is from Pimenidou and Dupont [68]
[b] Macro-families are based on Garcia-Perez[67]

Table 3 shows the key stoichiometric information for each feedstock in SE-CLSR (R11). Methane is also included for comparison, as it is a common steam reforming feedstock. The stoichiometry illustrates some key constraints, such as the potential hydrogen yield, required S/C ratio and appropriate quantities of OTM and sorbent.

Table 3 - Summary of stoichiometry for SE-CLSR of methane, bio-oil model compounds, and PEFB bio-oil surrogate mixture (Reaction 11)

		Methane	**Acetic acid**	**Furfural**	**PEFB bio-oil (moisture-free)**
Composition ($C_nH_mO_k$)	n	1	2	5	4.057
	m	4	4	4	4.977
	k	0	2	2	1.776
Molar mass (kg/kmol)		16.05	60.06	96.09	82.17
Reactants ($mol_i\ mol_{feedstock}^{-1}$)	NiO	1.000	0.667	3.667	2.873
	H_2O	1.000	1.333	4.333	3.465
	CaO	1.000	2.000	5.000	4.057
Products ($mol_i\ mol_{feedstock}^{-1}$)	Ni	1.000	0.667	3.667	2.873
	$CaCO_3$	1.000	2.000	5.000	4.057
	H_2	3.000	3.333	6.333	5.954
S/C ratio		1.000	0.667	0.867	0.854
NiO/C ratio		1.000	0.333	0.733	0.708
CaO/C ratio		1.000	1.000	1.000	1.000
$mol_{H2}\ mol_{carbon}^{-1}$		3.000	1.667	1.267	1.468

4. Results and discussion

4.1. Process comparison and effect of temperature

Fig. 2 shows the performance of each process over a range of temperatures and at atmospheric pressure. Fig. 2a and Fig. 2b indicate that the sorbent enhances the yield and purity of C-SR and CLSR, until the sorbent becomes ineffective at around 1050K. At certain temperatures, the sorption

enhanced processes achieve purity over 99mol%, while C-SR and CLSR only reach 60mol% purity, and would require extensive downstream processing.

In SE-CLSR with S/C ratio of 2, maximum H_2 yield (11.7 wt%) is achieved at 823K, at which point the purity is 99.6mol% H_2, with 0.2 mol% CO_2, 0.1 mol% CH_4 and 0.05 mol% CO. However, maximum purity (99.7 mol%) is achieved at 723K, where yield is slightly lower than the maximum (11.6 wt%). The remaining 0.3% is methane, and other impurities are negligible (<1ppm). To reduce the requirement for downstream processing, the optimal operating point is likely to be the point of maximal purity, where yield will be slightly lower than the maximum.

As result of the enhanced yield, SE-SR has a lower net energy balance than C-SR, despite the requirement for heat to regenerate the sorbent (Fig. 2c). At atmospheric pressure, SE-CLSR has a lower net energy balance than CLSR only between the range of around 800 – 1050 K. This can be explained by the individual energy terms, shown in Fig. 3. Below 800K, the CLSR energy balance is dominated by the oxidation term. Both CLSR and SE-CLSR release the same quantity of heat in oxidation but CLSR has a very low yield in this region, so that the energy released per mole of H_2 is higher. While CLSR appears to have a thermodynamic advantage over SE-CLSR at this point, it is unlikely that the process would be operated in this region as the yield is low. Above 1050K, the calcium sorbent becomes ineffective and so both CLSR and SE-CLSR have the same net energy balance. The design of advanced reforming processes should consider these interactions between yield and heating burden in order to find an optimal balance.

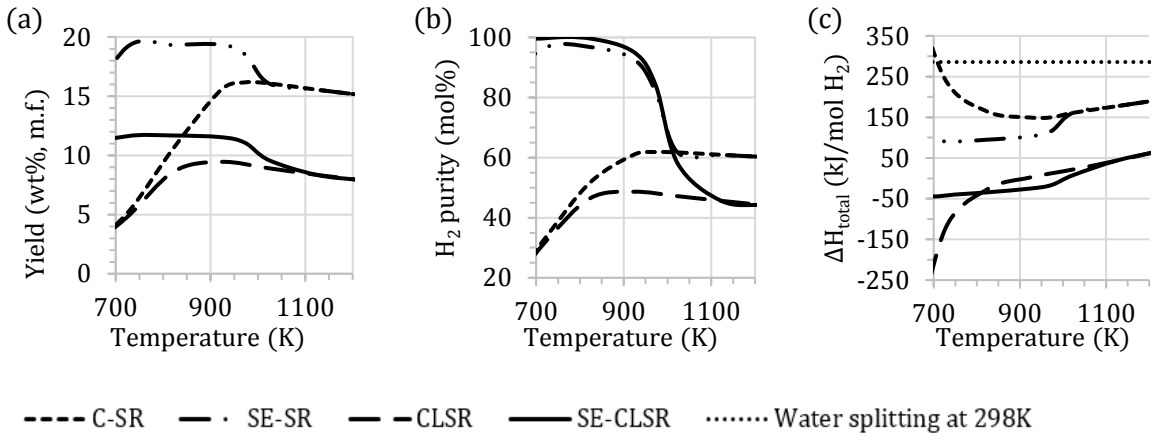

Fig. 2 - The effect of reduction/reforming temperature (T_1) for PEFB bio-oil surrogate mixture in C-SR, CLSR, SE-SR and SE-CLSR with S/C ratio of 2 at 1.013 bar. For SE-SR and SE-CLSR, CaO/C = 1 and NiO/C = 1. **(**a) mass yield, moisture-free basis, (b) H_2 purity, (c) net process energy balance.

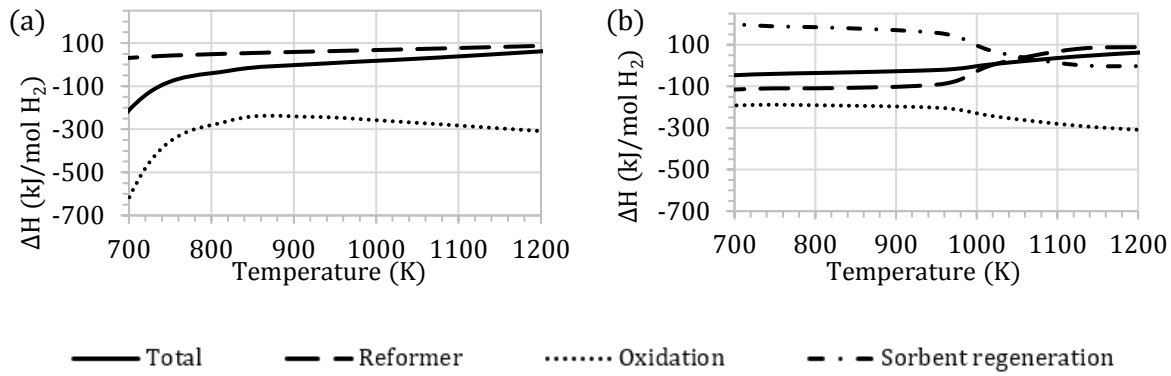

Fig. 3 - The effect of reduction/reforming temperature (T_1) on the main energy terms in advanced reforming of PEFB bio-oil surrogate mixture with S/C = 2 at 1.013 bar (a) CLSR, with NiO/C = 1 and CaO/C = 0, (b) SE-CLSR, with NiO/C = 1 and CaO/C = 1.

The equilibrium yields for the PEFB bio-oil mixture are similar to yields observed in experimental studies. Remón et al. [60] measured steam reforming yields in the range of 10 to 18 wt% from various bio-oils at S/C = 7.6 and 923K. At the same conditions, the C-SR equilibrium model gives 11.6 wt% m.f. For a real PEFB bio-oil, Zin et al. [71] measured a yield of 9.5 wt% m.f. with S/C = 2.75 at 873K. Sorption enhancement increased the yield to 10.4 wt%, with H_2 purity of 97%. At the same conditions, the model gives 16.2 wt% m.f and 21.1 wt% m.f. in SR and SE-SR respectively. A direct comparison is not applicable as the molecular composition was different in each case. Nonetheless, these figures indicate that the surrogate mixture gives predictions within a reasonable range.

Experimental demonstration of advanced reforming of bio-oil is more limited, but there is some evidence of model compounds achieving close to equilibrium yield in CLSR. In CLSR at 923K, acetic acid achieved 7.13 wt%, or 61.27% of equilibrium yield, while furfural achieved 12.6 wt%, or 71.86% of equilibrium yield [47].

One limitation of thermodynamic analysis is that it does not represent the deactivation of OTM and sorbent over multiple cycles. Acetic acid has displayed stable performance over at least 10 successive cycles in CLSR and SE-CLSR, with carbon deposits being removed during the oxidation stage [39,43]. However, a whole bio-oil may display different deactivation behaviour. Catalyst stability is not within the scope of this study, but it is an important consideration for future work on process feasibility.

4.2. Feedstock comparison in the SE-CLSR process

The previous section focussed on bio-oil surrogate mixture, but it is also useful to understand how common model compounds perform in the same analysis. Fig. 4 shows the yield and net energy balance for each feedstock in SE-CLSR.

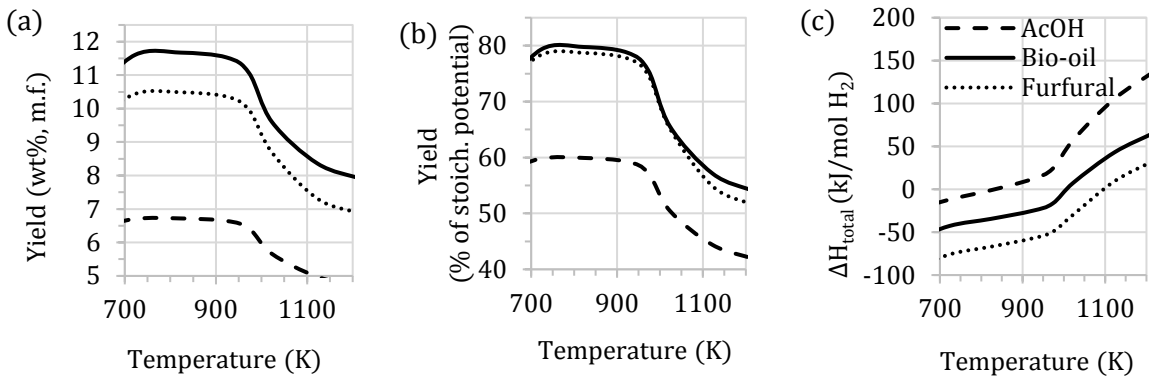

Fig. 4 - The effect of reduction/reforming temperature (T_1) in SE-CLSR of acetic acid, bio-oil and furfural at 1.013 bar with S/C = 2, NiO/C = 1, CaO/C = 1 (a) mass yield, moisture-free basis, (b) yield in % of stoichiometric potential from the SE-CLSR global reaction, (c) yield in mol H_2 product per mol of H_2 in feedstock, (d) net process energy balance

Fig. 4a shows the mass yield, as this parameter is commonly used for reporting experimental results in bio-oil reforming. The mass yield from bio-oil peaks at 11.7 wt% m.f., while acetic acid achieves only 6.7 wt% m.f. This is explained by the stoichiometry in Table 3. Although bio-oil has a higher molar mass (i.e. a higher denominator), this is balanced by a high molar yield. When the stoichiometric yield is used (Fig. 4b), bio-oil and furfural are closely matched due to the similarity in their chemical formula shown in Table 3 ($C_nH_mO_k$). The behaviour of furfural more closely models that of the bio-oil, suggesting that it is a more suitable model compound for representing the performance of bio-oil.

Figure 4c shows the wide variation in net energy balance between the different feedstocks. At the range of conditions considered, the furfural energy balance is lower than that of bio-oil, by 32 to 37 kJ mol_{H2}^{-1}. The net energy balance for acetic acid is higher than that of bio-oil, by 30 to 72 kJ mol_{H2}^{-1}. In the optimal region, both model compounds are a similar distance from the bio-oil mixture. This highlights that variations in bio-oil composition could have a large impact on the energy balance, so that feedstock variation would be an important factor in process design and control.

These results were generated using the same NiO/C ratio (NiO/C = 1). In practice, each feedstock will have a different optimal NiO/C ratio, according to the reaction stoichiometry (Table 3). For example, acetic acid appears to be performing well beneath its stoichiometric potential in Figure 4b, but this is because NiO/C of 1 represents a large excess of NiO above the required level (0.333). Thus, it is not appropriate to make a direct comparison of feedstocks at a single set of conditions. Instead, the process should be optimised, and the different optimal solutions compared. Section 4.4 examines this optimisation.

4.3. Carbon deposition

At S/C ratio of 2 and above, the results showed no carbon deposition in bio-oil steam reforming. A high excess of steam inhibits carbon deposition, and enables steam gasification of any existing

carbon deposits [41]. However, operating with a lower S/C may be preferable as it reduces the process energy balance. Section 4.4 contains further detail on the influence of S/C ratio on yield and energy balance. To understand the risk of carbon deposition at low S/C ratios, Fig. 5 shows solid carbon yields with S/C = 1.

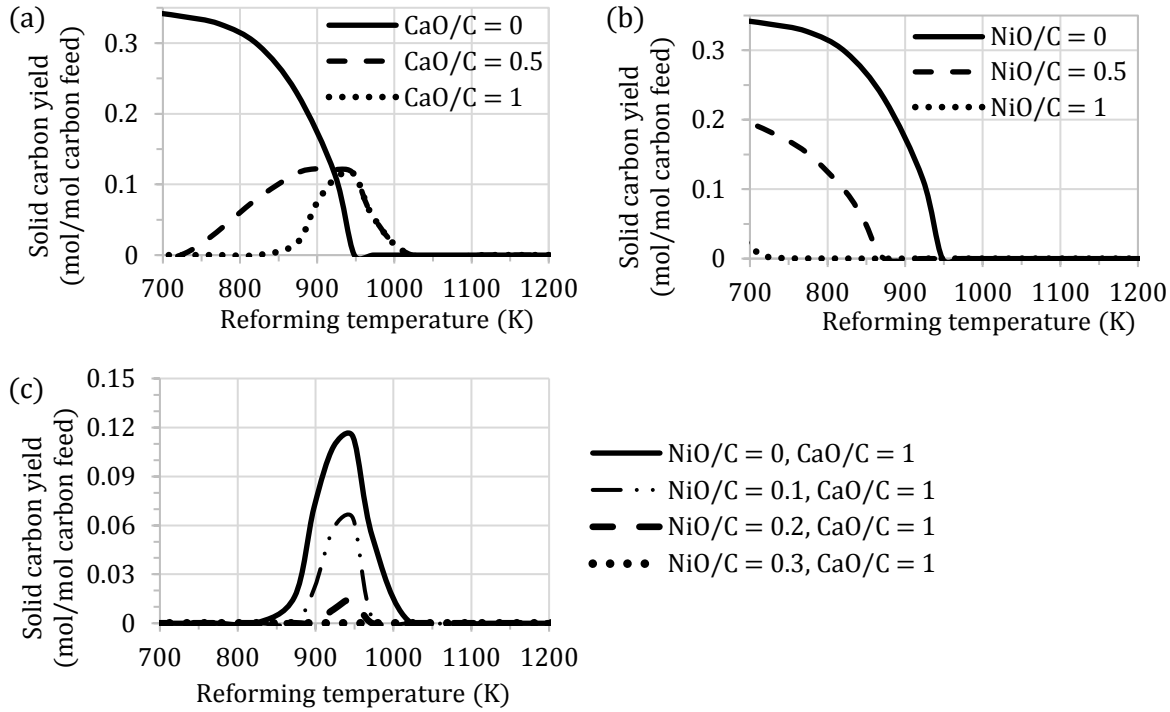

Fig. 5 - Equilibrium carbon product in the advanced reforming of PEFB bio-oil surrogate mixture with S/C =1 at 1.013 bar (a) SE-SR, with NiO/C = 0, (b) CLSR, with CaO/C = 0, (c) SE-CLSR, with CaO/C = 1.

In SE-SR, the presence of sorbent changes the limit for carbon deposition (Fig. 5a). The upper temperature limit is increased, but a minimum temperature is also introduced, to give an envelope in which equilibrium carbon product occurs. As more sorbent is introduced, the lower limit increases so that the envelope for carbon deposition is narrowed. In SE-SR with a stoichiometric quantity of sorbent (CaO/C = 1), carbon deposition occurs between 823K and 973K. Previous thermodynamic studies have similarly found that carbon deposition is suppressed by CO_2 sorption. These studies suggest that the enhanced WGS reaction reduces CO content, and thus shifts the equilibrium for the Boudouard reaction (R14) backwards [72,73].

Figure 5b shows the effect of OTM content in CLSR. Increasing the amount of NiO moves the temperature boundary for carbon, so that carbon is eliminated at lower temperatures. By increasing NiO/C to 1, carbon product is eliminated at any temperature over 725K. This is the result of introducing oxygen into the reactor, which enables the oxidation of carbon.

The combined effects of both OTM and sorbent in SE-CLSR are shown in Figure 5c. With CaO/C =1, and S/C = 1, carbon product is eliminated with NiO/C of 0.3 or above. These results highlight a potential advantage of SE-CLSR: by combining the effects of the sorbent and OTM, carbon can be supressed to very low levels across a wide operating range.

4.4. Optimisation and autothermal operation in SE-CLSR of bio-oil

The analysis has highlighted that the process is affected by several interacting parameters which should be considered together. As well as temperature and pressure, other key parameters for consideration are the ratios S/C, NiO/C and CaO/C. These parameters can be manipulated to enhance yield and purity, reduce energy demand and eliminate carbon deposition.

In this optimisation study of H_2 production from bio-oil, three parameters are initially fixed: pressure, temperature, and CaO/C ratio. According to Le Chatelier's principle, the reaction is favoured by low pressures, so the pressure is fixed at 1.013 bar. Temperature is fixed at 723K. The earlier analysis identified that this temperature maximises purity and gives close to maximum yield at this pressure.

Fig. 6 shows the effect of CaO/C ratio in SE-CLSR. According to the stoichiometry (Table 3), CaO/C = 1 provides enough sorbent to capture all of the CO_2. Increasing CaO beyond this point does not increase the yield (Fig. 6a), but simply increases the net energy balance and expense associated with excess sorbent. For this reason, the amount of sorbent is fixed at CaO/C = 1.

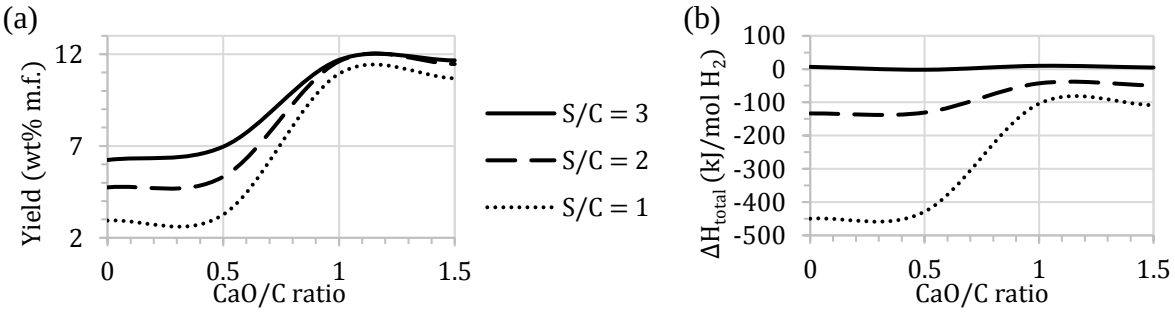

Fig. 6 - Effect of sorbent in SE-CLSR of bio-oil at 1.013 bar and 723K, with NiO/C = 1 (a) mass yield, moisture-free basis (b) net process energy balance.

The effects of NiO/C ratio and S/C ratio are illustrated in Fig. 7. Fig. 7b shows that the net energy balance can be reduced by increasing NiO/C ratio, as more heat is released from the oxidation of fuel and Ni. Above a certain NiO/C ratio, autothermal operation ($\Delta H \leq 0$) is theoretically possible. However, the reduced energy balance comes at the cost of lower H_2 yield (Fig. 7a). Similarly, lower S/C ratio reduces heat demand, but also decreases H_2 yield and purity. For S/C = 1, the purity is considerably reduced due to methanation. The selection of NiO/C ratio and S/C ratio should balance the conflicting objectives.

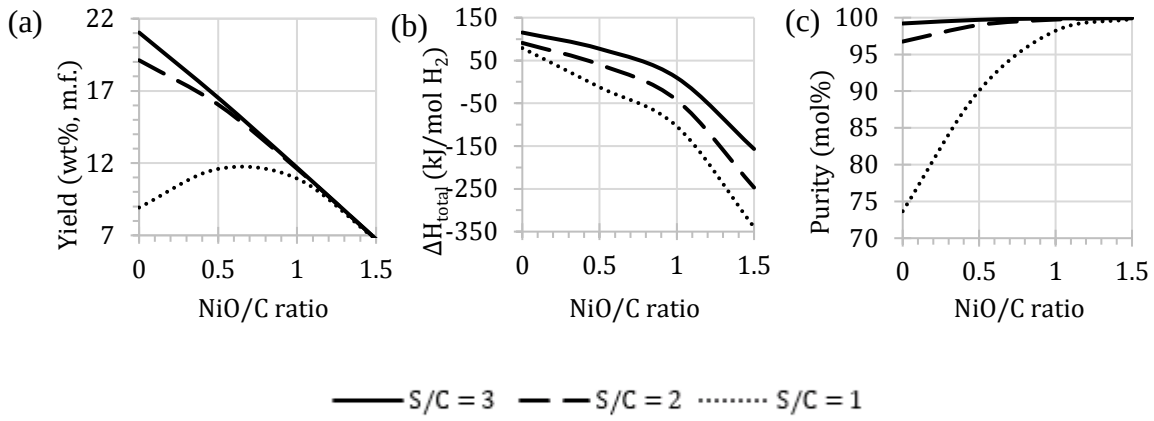

Fig. 7 - Effect of OTM in SE-CLSR of bio-oil at 1.013 bar and 723K, with CaO/C = 1 (a) mass yield, moisture-free basis, (b) net energy balance, (c) hydrogen purity.

Table 4 shows the autothermal point for the bio-oil surrogate mixture, as well as the model compounds acetic acid and furfural at 723K. In autothermal SE-CLSR of bio-oil, CO_2 and CO are reduced to a negligible level, so that downstream purification requirements are minimised.

A low quantity of steam (S/C = 1) allows a small NiO inventory in autothermal operation, but also supports methanation, so that H_2 purity is low and over 12 mol% of the product gas is CH_4. By increasing the S/C ratio to 2, autothermal operation can be achieved alongside a high yield (13.6 wt%) and minimal methanation.

When comparing feedstocks, it is notable that the optimal solution for a bio-oil mixture is different to that of the model compounds. As seen in earlier results, furfural is a closer match to bio-oil and thus is a more suitable model compound for understanding thermodynamic potential. However, process development should aim to consider realistic bio-oil mixtures wherever possible.

Table 4 - Parameters for autothermal operation in SE-CLSR of bio-oil, acetic acid and furfural at 1.013 bar, 723K, with CaO/C = 1. In all cases, solid carbon and CO are negligible (<1ppm)

Feedstock	S/C	Minimum NiO/C	Yield (wt%, m.f.)	Yield (wt%, wet)	H_2 purity (mol%)	CO_2 (mol%)	CH_4 (mol%)
Bio-oil	3	1.050	11.2	8.51	99.95	0	0.0536
	2	0.785	13.6	10.3	99.52	0	0.482
	1	0.419	11.3	8.59	87.91	0	12.1
Acetic acid	3	1.210	5.31	-	99.94	0.0633	0
	2	0.949	7.04	-	99.99	0	0
	1	0.679	8.49	-	98.86	0	1.14
Furfural	3	0.940	11.1	-	99.91	0.0189	0.0756
	2	0.675	13.6	-	99.43	0.0153	0.552
	1	0.267	9.22	-	80.36	0	19.6

While it may be possible to design an autothermal process, this comes at the expense of a reduced yield (Fig. 7). Hence the preferred operating regime will depend on whether autothermal operation is a priority, which will depend on plant-specific constraints such as required capacity, and the availability and cost of heat. Further techno-economic analysis would be required to find the optimal solution for a given plant, but the above method of thermodynamic analysis could be a valuable starting point for such an evaluation.

4.5. Heat recuperation

The analysis above assumes that usable heat is recovered from both solids and gases after the oxidation/regeneration stage. Fig. 8 shows the impact on the energy balance if the heat recuperation terms are not included. Recuperation of heat from the gas has the largest impact. The impact of heat recuperation from solids decreases when the temperature of reduction/reforming approaches the same temperature as regeneration/oxidation (1170K). When combined, both types of recuperation reduce the net energy balance by 60 to 115 kJ mol_{H2}^{-1}.

This highlights the importance of heat integration in SE-CLSR. As the process is cyclical, parts of the process are repeatedly heated and cooled, and there is the potential to waste a large amount of heat if process design does not consider heat integration. Previous work has highlighted that the catalyst support can introduce a large additional heating burden[41], which would further increase the impact of heat recuperation from the solids.

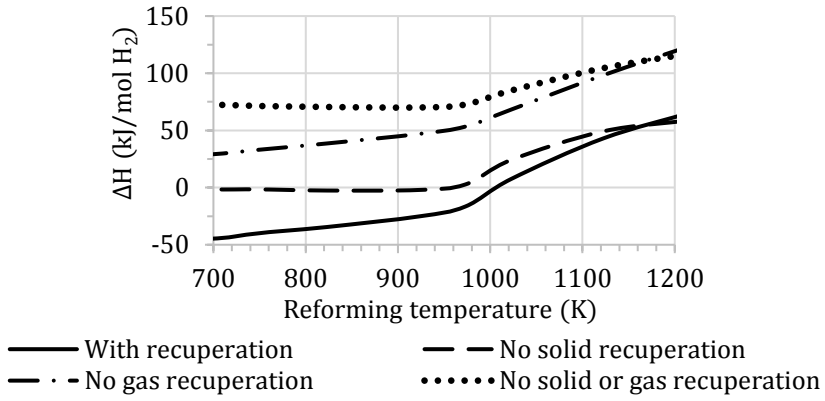

Fig. 8 - Effect of heat recuperation in SE-CLSR of bio-oil at 1.01325 bar, with S/C = 1, CaO/C = 1, NiO/C = 1.

4.6. The effect of pressure on SE-CLSR

Low pressure favours the production of hydrogen in the steam reforming reaction. However, industrial reforming processes are typically operated at high pressures, in the region of 20 bar or higher, to enable efficient processing of large gas flows in reduced reactor and pipe volumes [74]. Fig. 9 illustrates how the various reforming processes are affected by elevated pressures.

As pressure is increased, the maximum H_2 yield is slightly decreased, and occurs at a higher temperature. At atmospheric pressure, the maximum yield is 11.6 wt% at 723K. At 30 bar, maximum yield is 10.9 wt% at 1023K (Fig. 9a). Fig. 9b shows that purity over 90 mol% is achievable at all the studied pressures, due to the CO_2 sorbent. However, as pressure increases the maximum purity is lowered, and the region of maximum purity is narrowed. In a 30 bar system, H_2 purity peaks at 96.7 mol%. The main impurity is CH_4 (1.8 mol%), as the high pressure system is favourable for methanation (R4 and R5). The level of methanation is illustrated in Fig. 9c.

To achieve a given H_2 yield, the high pressure system requires a higher reformer temperature. However, Fig. 9d shows that the net process energy balance remains similar. In the low temperature region, higher pressure leads to more methanation (Fig. 9c), which releases heat into the reformer. In the high temperature region, the energy balance is affected by the sorption reaction – as the sorbent becomes ineffective, it no longer provides heat for sorption. This effect is observed at lower temperatures in low pressure systems.

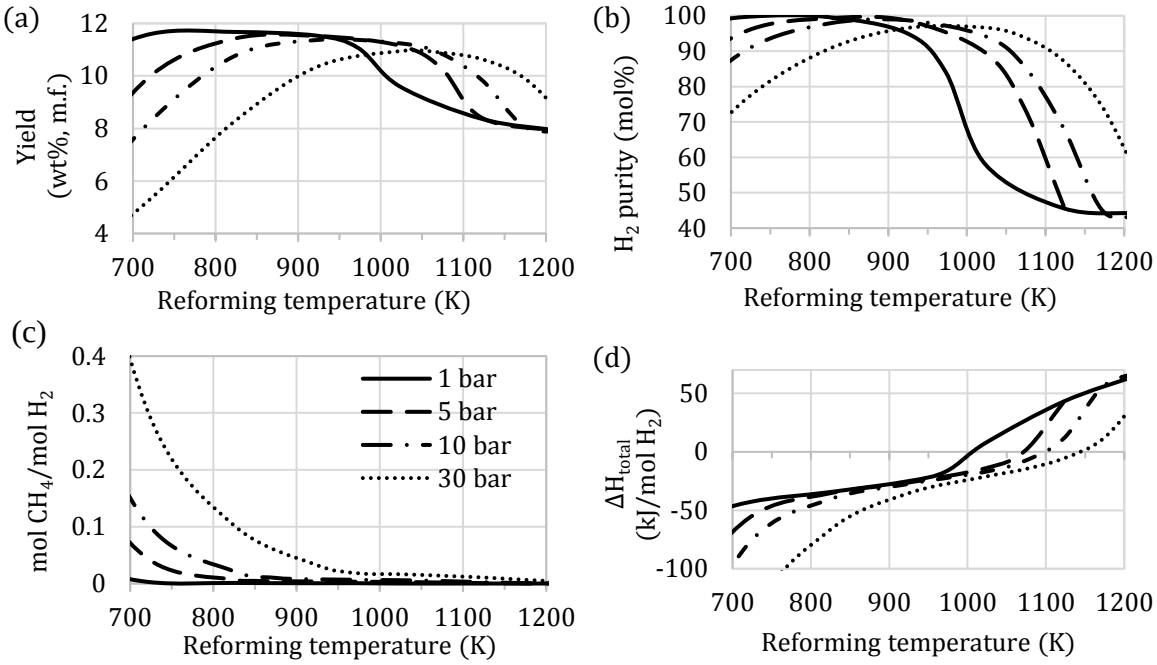

Fig. 9 - Effect of pressure in SE-CLSR of bio-oil, with S/C = 2, NiO/C = 1, CaO/C = 1 (a) mass yield, moisture-free basis, (b) hydrogen purity, (c) methane production, (d) net process energy balance.

Table 5 gives parameters for autothermal operation at elevated pressures. Autothermal operation remains a possibility at industrial reforming pressures, but the higher pressure leads to a higher NiO inventory, reduced yield, and more impurities.

Table 5 - Parameters for autothermal operation in SE-CLSR of bio-oil, at various pressures with CaO/C = 1. In all cases, solid carbon yield is negligible.

Pressure (bar)	S/C (-)	T (K)	Minimum NiO/C	Yield (wt%, m.f.)	Yield (wt%, wet)	H_2 purity (mol%)	CO (mol%)	CO_2 (mol%)	CH_4 (mol%)
30	3	973	1.189	9.68	7.36	98.7	0.183	0.795	0.367
	2	973	0.867	11.8	8.95	96.9	0.197	0.346	2.57
	1	973	0.424	8.19	6.23	77.6	0.341	0.227	21.9
10	3	873	1.134	10.3	7.82	99.5	0.0580	0.232	0.232
	2	873	0.835	12.6	9.55	98.3	0.0469	0.0939	1.60
	1	873	0.418	9.20	6.99	81.5	0.0531	0.0531	18.4
5	3	848	1.122	10.5	7.96	99.7	0	0.171	0.114
	2	848	0.834	13.0	9.85	99.1	0.0456	0.0917	0.779
	1	848	0.427	9.94	7.55	84.1	0.0507	0.0507	15.8

5. Conclusion

A thermodynamic evaluation has demonstrated the potential of bio-oil steam reforming and highlighted the role of advanced reforming techniques in enhancing its performance. Sorption

enhancement can increase hydrogen yield and purity, while also decreasing the net process energy balance. Chemical looping reduces energy balance, although hydrogen yield is reduced due to the partial oxidation of the feedstock. When both techniques are combined in SE-CLSR, bio-oil can be converted to hydrogen in a process with purity over 99% and a low net energy balance.

A PEFB bio-oil surrogate mixture has been compared to model compounds acetic acid and furfural. Due to the similarity in molecular formula, furfural is a more representative model compound for whole PEFB bio-oil. The comparison also highlighted that the feedstock has a considerable impact on process energy balance, and as such process design should consider the variability of bio-oil compositions.

The SE-CLSR of bio-oil can achieve autothermal operation with yields over 13wt% and purity over 99.5 mol%, so that it may be possible to develop small bio-oil reforming plants which are energy self-sufficient and require minimal product purification. Autothermal operation is also achievable at industrial reforming pressures, although the product yield and purity are reduced. The recuperation of heat from solid materials and waste gases is a major contributor to the energy balance. Heat integration is therefore a key consideration for process development.

Carbon deposition is present when S/C ratio is low (S/C = 1), but the risk of carbon product can be reduced by increasing the quantity of OTM or sorbent. The autothermal operating regimes for SE-CLSR showed no solid carbon in the equilibrium products.

Thermodynamic analysis demonstrates how advanced reforming techniques can improve the potential of bio-oil as a low-carbon feedstock for hydrogen, in theory improving cost-effectiveness and flexibility of scale in low carbon hydrogen production. This study used a high-level overview of reactor thermodynamics, but further work is required to assess the feasibility of a real process, taking into account practical aspects such as auxiliary units, heat transfer, and the approach to heat integration. Economic constraints are another important consideration. Further process development is required, including the use of techno-economic analysis to evaluate economic feasibility and optimisation.

Acknowledgements

The Engineering and Physical Sciences Research Council is gratefully acknowledged for supporting this work, via Jennifer Spragg's studentship in the Centre for Doctoral Training in Bioenergy [grant number EP/L014912/1]. We are also grateful to the UKCCSRC EPSRC consortium for Call 2 grant 'Novel Materials and Reforming Process Route for the Production of Ready-Separated CO2/N2/H2 from Natural Gas Feedstocks' [grant number EP/ K000446/1]. Data associated with this publication are available under a CC-BY license at https://doi.org/10.5518/451.

Declarations of interest

The authors declare no conflict of interest.

References

[1] Milne TA, Elam CC, Evans RJ. Hydrogen from biomass: state of the art and research challenges. 2002. doi:10.2172/792221.

[2] Díaz-González F, Sumper A, Gomis-Bellmunt O, Villafáfila-Robles R. A review of energy storage technologies for wind power applications. Renew Sustain Energy Rev 2012;16:2154–71. doi:10.1016/j.rser.2012.01.029.

[3] Dodds PE, McDowall W. The future of the UK gas network. Energy Policy 2013;60:305–16. doi:10.1016/j.enpol.2013.05.030.

[4] Ball M, Weeda M. The hydrogen economy - Vision or reality? Int J Hydrogen Energy 2015;40:7903–19. doi:10.1016/j.ijhydene.2015.04.032.

[5] IEA. Technology Roadmap - Hydrogen and Fuel Cells 2015.

[6] Marbán G, Valdés-Solís T. Towards the hydrogen economy? Int J Hydrogen Energy 2007;32:1625–37. doi:10.1016/j.ijhydene.2006.12.017.

[7] Chen B, Liao Z, Wang J, Yu H, Yang Y. Exergy analysis and CO2 emission evaluation for steam methane reforming. Int J Hydrogen Energy 2012;37:3191–200. doi:10.1016/j.ijhydene.2011.10.102.

[8] Ozbilen A, Dincer I, Rosen MA. Comparative environmental impact and efficiency assessment of selected hydrogen production methods. Environ Impact Assess Rev 2013;42:1–9. doi:10.1016/j.eiar.2013.03.003.

[9] Le Quéré C, Andrew RM, Friedlingstein P, Sitch S, Pongratz J, Manning AC, et al. Global Carbon Budget 2017. Earth Syst Sci Data 2018;10:405–48. doi:10.5194/essd-10-405-2018.

[10] Acar C, Dincer I. Impact assessment and efficency evaluation of hydrogen production methods. Int J Chem React Eng 2015;39:1757–68. doi:10.1002/er.3302.

[11] Heracleous E. Well-to-Wheels analysis of hydrogen production from bio-oil reforming for use in internal combustion engines. Int J Hydrogen Energy 2011;36:11501–11. doi:10.1016/j.ijhydene.2011.06.052.

[12] Trane R, Dahl S, Skjøth-Rasmussen MS, Jensen AD. Catalytic steam reforming of bio-oil. Int J Hydrogen Energy 2012;37:6447–72. doi:10.1016/j.ijhydene.2012.01.023.

[13] Chen J, Sun J, Wang Y. Catalysts for Steam Reforming of Bio-oil: A Review. Ind Eng Chem Res 2017;56:4627–37. doi:10.1021/acs.iecr.7b00600.

[14] Kumar A, Chakraborty JP, Singh R. Bio-oil: the future of hydrogen generation. Biofuels 2017;8:663–74. doi:10.1080/17597269.2016.1141276.

[15] Tzanetis KF, Martavaltzi CS, Lemonidou AA. Comparative exergy analysis of sorption enhanced and conventional methane steam reforming. Int J Hydrogen Energy 2012;37:16308–20. doi:10.1016/j.ijhydene.2012.02.191.

[16] Dou B, Wang C, Song Y, Chen H, Jiang B, Yang M, et al. Solid sorbents for in-situ CO2 removal during sorption-enhanced steam reforming process: A review. Renew Sustain Energy Rev 2016;53:536–46. doi:10.1016/j.rser.2015.08.068.

[17] Yancheshmeh MS, Radfarnia HR, Iliuta MC. High temperature CO2 sorbents and their application for hydrogen production by sorption enhanced steam reforming process. Chem Eng J 2016;283:420–44. doi:10.1016/j.cej.2015.06.060.

[18] García-Díez E, García-Labiano F, De Diego LF, Abad A, Gayán P, Adánez J. Autothermal chemical looping reforming process of different fossil liquid fuels. Int J Hydrogen Energy 2017;42:13633–40. doi:10.1016/j.ijhydene.2016.12.109.

[19] Adánez J, Abad A, García-Labiano F, Gayan P, De Diego LF. Progress in chemical-looping combustion and reforming technologies. Prog Energy Combust Sci 2012;38:215–82. doi:10.1016/j.pecs.2011.09.001.

[20] Luo M, Yi Y, Wang S, Wang Z, Du M, Pan J, et al. Review of hydrogen production using

chemical-looping technology. Renew Sustain Energy Rev 2018;81:3186–214. doi:10.1016/j.rser.2017.07.007.

[21] Voitic G, Hacker V. Recent advancements in chemical looping water splitting for the production of hydrogen. RSC Adv 2016;6:98267–96. doi:10.1039/c6ra21180a.

[22] Zeng D-W, Xiao R, Zhang S, Zhang H-Y. Bio-oil heavy fraction for hydrogen production by iron-based oxygen carrier redox cycle. Fuel Process Technol 2015;139:1–7. doi:10.1016/j.fuproc.2015.08.007.

[23] Zeng D-W, Xiao R, Huang Z, Zeng J-M, Zhang H-Y. Continuous hydrogen production from non-aqueous phase bio-oil via chemical looping redox cycles. Int J Hydrogen Energy 2016;41:6676–84. doi:10.1016/j.ijhydene.2016.03.052.

[24] Fathi M, Bjorgum E, Viig T, Rokstad OA. Partial oxidation of methane to synthesis gas: Elimination of gas phase oxygen. Catal Today 2000;63:489–97. doi:10.1016/S0920-5861(00)00495-8.

[25] Rydén M, Lyngfelt A, Mattisson T. Two novel approaches for hydrogen production, chemical-looping reforming and steam reforming with carbon dioxide capture by chemical-looping combustion. Fuel 2006;85:1631–41.

[26] Antzara A, Heracleous E, Silvester L, Bukur DB, Lemonidou AA. Activity study of NiO-based oxygen carriers in chemical looping steam methane reforming. Catal Today 2016;272:32–41. doi:10.1016/j.cattod.2015.10.027.

[27] Neal L, Shafiefarhood A, Li F. Effect of core and shell compositions on MeOx@LaySr1-yFeO3 core-shell redox catalysts for chemical looping reforming of methane. Appl Energy 2015;157:391–8. doi:10.1016/j.apenergy.2015.06.028.

[28] Ortiz M, De Diego LF, Abad A, García-Labiano F, Gayán P, Adánez J. Catalytic activity of ni-based oxygen-carriers for steam methane reforming in chemical-looping processes. Energy and Fuels 2012;26:791–800. doi:10.1021/ef2013612.

[29] Silvester L, Antzara A, Boskovic G, Heracleous E, Lemonidou AA, Bukur DB. NiO supported on Al2O3 and ZrO2 oxygen carriers for chemical looping steam methane reforming. Int J Hydrogen Energy 2015;40:7490–501. doi:10.1016/j.ijhydene.2014.12.130.

[30] Tang M, Xu L, Fan M. Progress in oxygen carrier development of methane-based chemical-looping reforming: A review. Appl Energy 2015;151:143–56. doi:10.1016/j.apenergy.2015.04.017.

[31] Pröll T, Bolhàr-Nordenkampf J, Kolbitsch P, Hofbauer H. Syngas and a separate nitrogen/argon stream via chemical looping reforming - A 140 kW pilot plant study. Fuel 2010;89:1249–56. doi:10.1016/j.fuel.2009.09.033.

[32] Rydén M, Ramos P. H2 production with CO2 capture by sorption enhanced chemical-looping reforming using NiO as oxygen carrier and CaO as CO2 sorbent. Fuel Process Technol 2012;96:27–36. doi:10.1016/j.fuproc.2011.12.009.

[33] Chen H, Zhang T, Dou B, Dupont V, Williams PT, Ghadiri M, et al. Thermodynamic analyses of adsorption-enhanced steam reforming of glycerol for hydrogen production. Int J Hydrogen Energy 2009;34:7208–22. doi:10.1016/j.ijhydene.2009.06.070.

[34] Dou B, Rickett GL, Dupont V, Williams PT, Chen H, Ding Y, et al. Steam reforming of crude glycerol with in situ CO2 sorption. Bioresour Technol 2010;101:2436–42. doi:10.1016/j.biortech.2009.10.092.

[35] Lea-Langton A, Giannakeas N, Rickett G, Dupont V, Twigg MV. Waste lubricating oil as a source of hydrogen fuel using chemical looping steam reforming. SAE Int J Fuels Lubr 2010;3:810–8.

[36] Cormos C-C. Renewable hydrogen production concepts from bioethanol reforming with carbon capture. Int J Hydrogen Energy 2014;39:5597–606. doi:10.1016/j.ijhydene.2014.01.114.

[37] Lea-Langton A, Zin RM, Dupont V, Twigg MV. Biomass pyrolysis oils for hydrogen production using chemical looping reforming. Int J Hydrogen Energy 2012;37:2037–43.

doi:http://dx.doi.org/10.1016/j.ijhydene.2011.05.083.

[38] Cheng F, Dupont V. Steam Reforming of Bio-Compounds with Auto-Reduced Nickel Catalyst. Catalysts 2017;7:114. doi:10.3390/catal7040114.

[39] Omoniyi OA, Dupont V. Chemical looping steam reforming of acetic acid in a packed bed reactor. Appl Catal B Environ 2018;226:258–68. doi:10.1016/j.apcatb.2017.12.027.

[40] Antzara A, Heracleous E, Lemonidou AA. Energy efficient sorption enhanced-chemical looping methane reforming process for high-purity H2 production: Experimental proof-of-concept. Appl Energy 2016;180:457–71. doi:10.1016/j.apenergy.2016.08.005.

[41] S G Adiya ZI, Dupont V, Mahmud T. Chemical equilibrium analysis of hydrogen production from shale gas using sorption enhanced chemical looping steam reforming. Fuel Process Technol 2017;159:128–44. doi:10.1016/j.fuproc.2017.01.026.

[42] Yahom A, Powell J, Pavarajarn V, Onbhuddha P, Charojrochkul S, Assabumrungrat S. Simulation and thermodynamic analysis of chemical looping reforming and CO2 enhanced chemical looping reforming. Chem Eng Res Des 2014;92:2575–83. doi:10.1016/j.cherd.2014.04.002.

[43] Omoniyi OA. Sorption enhancement and chemical looping as process intensificaiton measures for the steam reforming of acetic acid: A base-case for the enhanced steam reforming of pyrolysis oils. University of Leeds, n.d.

[44] IPCC. Summary for Policymakers. In: Edenhofer O, Pichs-Madruga R, Sokona Y, Farahani E, Kadner S, Seyboth K, et al., editors. Clim. Chang. 2014 Mitig. Clim. Chang. Contrib. Work. Gr. III to Fifth Assess. Rep. Intergov. Panel Clim. Chang., Cambridge, United Kingdom and New York, NY, USA: Cambridge University Press; 2014, p. 1–33. doi:10.1017/CBO9781107415324.

[45] Antzara A, Heracleous E, Bukur DB, Lemonidou AA. Thermodynamic analysis of hydrogen production via chemical looping steam methane reforming coupled with in situ CO2 capture. Energy Procedia 2014;63:6576–89. doi:10.1016/j.egypro.2014.11.694.

[46] Tippawan P, Thammasit T, Assabumrungrat S, Arpornwichanop A. Using glycerol for hydrogen production via sorption-enhanced chemical looping reforming: Thermodynamic analysis. Energy Convers Manag 2016;124:325–32. doi:10.1016/j.enconman.2016.07.018.

[47] Cheng F. Bio-Compounds as Reducing Agents of Reforming Catalyst and their Subsequent Steam Reforming Performance. The University of Leeds, 2014.

[48] Goicoechea S, Ehrich H, Arias PL, Kockmann N. Thermodynamic analysis of acetic acid steam reforming for hydrogen production. J Power Sources 2015;279:312–22. doi:10.1016/j.jpowsour.2015.01.012.

[49] Tian X, Wang S, Zhou J, Xiang Y, Zhang F, Lin B, et al. Simulation and exergetic evaluation of hydrogen production from sorption enhanced and conventional steam reforming of acetic acid. Int J Hydrogen Energy 2016;41:21099–108. doi:10.1016/j.ijhydene.2016.09.184.

[50] Xie H, Yu Q, Wang K, Shi X, Li X. Thermodynamic Analysis of Hydrogen Production from Model Compounds of Bio-oil Through Steam Reforming. Environ Sci Technol 2014;33:1008–16. doi:10.1002/ep.11846.

[51] Fernández JR, Abanades JC, Murillo R. Modeling of sorption enhanced steam methane reforming in an adiabatic fixed bed reactor. Chem Eng Sci 2012;84:1–11. doi:10.1016/j.ces.2012.07.039.

[52] Dupont V, Ross AB, Knight E, Hanley I, Twigg MV. Production of hydrogen by unmixed steam reforming of methane. Chem Eng Sci 2008;63:2966–79. doi:10.1016/j.ces.2008.02.015.

[53] Lan P, Xu QL, Lan LH, Ren ZW, Zhang SP, Yan YJ. A Model for Carbon Deposition During Hydrogen Production by the Steam Reforming of Bio-oil. Energy Sources, Part A Recover Util Environ Eff 2013;36:250–8. doi:10.1080/15567036.2012.754516.

[54] Aspen Technology Inc. Aspen Plus v8.8 Help n.d.

[55] Liu C, Wang H, Karim AM, Sun J, Wang Y. Catalytic fast pyrolysis of lignocellulosic biomass. Chem Soc Rev 2014;43:7594–623. doi:10.1039/C3CS60414D.

[56] Bimbela F, Oliva M, Ruiz J, García L, Arauzo J. Hydrogen production by catalytic steam reforming of acetic acid, a model compound of biomass pyrolysis liquids. J Anal Appl Pyrolysis 2007;79:112–20. doi:10.1016/j.jaap.2006.11.006.

[57] Galdámez JR, García L, Bilbao R. Hydrogen Production by Steam Reforming of Bio-Oil Using Coprecipitated Ni - Al Catalysts. Acetic Acid as a Model Compound. Energy & Fuels 2005;19:1133–42. doi:10.1021/ef049718g.

[58] Vagia EC, Lemonidou AA. Thermodynamic analysis of hydrogen production via autothermal steam reforming of selected components of aqueous bio-oil fraction. Int J Hydrogen Energy 2008;33:2489–500. doi:10.1016/j.ijhydene.2008.02.057.

[59] Wang D, Czernik S, Montane D, Mann M, Chornet E. Biomass to Hydrogen via Fast Pyrolysis and Catalytic Steam Reforming of the Pyrolysis Oil or Its Fractions. Abstr Pap Am Chem Soc 1997;36:1507–18. doi:10.1021/ie960396g.

[60] Remón J, Broust F, Volle G, García L, Arauzo J. Hydrogen production from pine and poplar bio-oils by catalytic steam reforming. Influence of the bio-oil composition on the process. Int J Hydrogen Energy 2015;40:5593–608. doi:10.1016/j.ijhydene.2015.02.117.

[61] Plou J, Lachén J, Durán P, Herguido J, Peña JA. Pure hydrogen from lighter fractions of bio-oil by steam-iron process: Effect of composition of bio-oil, temperature and number of cycles. Fuel 2017;203:452–9. doi:10.1016/j.fuel.2017.04.127.

[62] Sarkar S, Kumar A. Large-scale biohydrogen production from bio-oil. Bioresour Technol 2010;101:7350–61. doi:10.1016/j.biortech.2010.04.038.

[63] Zhang Y, Brown TR, Hu G, Brown RC. Comparative techno-economic analysis of biohydrogen production via bio-oil gasification and bio-oil reforming. Biomass and Bioenergy 2013;51:99–108. doi:10.1016/j.biombioe.2013.01.013.

[64] Medrano JA, Oliva M, Ruiz J, García L, Arauzo J. Hydrogen from aqueous fraction of biomass pyrolysis liquids by catalytic steam reforming in fluidized bed. Energy 2011;36:2215–24. doi:10.1016/j.energy.2010.03.059.

[65] Tande LN, Dupont V. Autothermal reforming of palm empty fruit bunch bio-oil: thermodynamic modelling. AIMS Energy 2016;4:68–92. doi:10.3934/energy.2016.1.68.

[66] Dupont V, Abdul Halim Yun H, White R, Tande LN. High methane conversion efficiency by low temperature steam reforming of bio-feedstock. REGATEC 2017, Verona, Italy: 2017.

[67] Garcia-Perez M, Chaala A, Pakdel H, Kretschmer D, Roy C. Characterization of bio-oils in chemical families. Biomass and Bioenergy 2007;31:222–42. doi:10.1016/j.biombioe.2006.02.006.

[68] Pimenidou P, Dupont V. Characterisation of palm empty fruit bunch (PEFB) and pinewood bio-oils and kinetics of their thermal degradation. Bioresour Technol 2012;109:198–205. doi:10.1016/j.biortech.2012.01.020.

[69] Abdul Halim Yun H, Dupont V. Thermodynamic analysis of methanation of palm empty fruit bunch (PEFB) pyrolysis oil with and without in situ CO_2 sorption. AIMS Energy 2015;3:774–97. doi:10.3934/energy.2015.4.774.

[70] Tande LN. Autothermal reforming of bio-oil model compounds. University of Leeds, 2018.

[71] Zin RM, Lea-Langton A, Dupont V, Twigg M V. High hydrogen yield and purity from palm empty fruit bunch and pine pyrolysis oils. Int J Hydrogen Energy 2012;37:10627–38. doi:10.1016/j.ijhydene.2012.04.064.

[72] Li M. Thermodynamic analysis of adsorption enhanced reforming of ethanol. Int J Hydrogen Energy 2009;34:9362–72. doi:10.1016/j.ijhydene.2009.09.054.

[73] Lima Da Silva A, Müller IL. Hydrogen production by sorption enhanced steam reforming of oxygenated hydrocarbons (ethanol, glycerol, n-butanol and methanol): Thermodynamic

modelling. Int J Hydrogen Energy 2011;36:2057–75. doi:10.1016/j.ijhydene.2010.11.051.

[74] Chaubey R, Sahu S, James OO, Maity S. A review on development of industrial processes and emerging techniques for production of hydrogen from renewable and sustainable sources. Renew Sustain Energy Rev 2013;23:443–62. doi:10.1016/j.rser.2013.02.019.